THE JOURNAL OF PHYSICAL CHEMISTRY A

ARTICLE

pubs.acs.org/JPCA

Excited States in Electron-Transfer Reaction Products: Ultrafast Relaxation Dynamics of an Isolated Acceptor Radical Anion

Daniel A. Horke, Gareth M. Roberts, and Jan R. R. Verlet*

Department of Chemistry, University of Durham, South Road, Durham, DH1 3LE, United Kingdom

Supporting Information

ABSTRACT: The spectroscopy and ultrafast relaxation dynamics of excited states of the radical anion of a representative charge-transfer acceptor molecule, 2,3,5,6-tetrafluoro-7,7,8,8-tetracyanoquinodimethane, have been studied in the gas phase using time-resolved photoelectron spectroscopy. The photoelectron spectra reveal that at least two anion excited states are bound. Time-resolved studies show that both excited states are very short-lived and internally convert to the anion ground state, with the lower energy state relaxing within 200 fs and a near-threshold valence-excited state relaxing on a 60 fs time scale. These excited states, and in particular the valence-excited state, present efficient pathways for electron-transfer reactions in the highly exergonic inverted region which commonly displays rates exceeding predictions from electron-transfer theory.

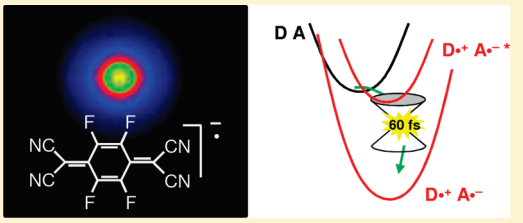

1. INTRODUCTION

Electron-transfer (ET) reactions, involving the transfer of an electron from a donor (D) to an acceptor (A) molecule, are among the most fundamental chemical reactions. They are of critical importance in many chemical and biological systems, including the key steps of photosynthesis,[1,2] energy conversion,[3] and metabolism.[4] They define the field of redox and electrochemistry and have paved the way for solid state electronics[5] and molecular electronics, the success of which will depend upon our understanding of the underlying ET processes.[6]

According to Marcus theory,[7] the ET is driven by the overall exergonicity of the reaction. As $\Delta G°$ becomes more negative, the reaction barrier diminishes with a concomitant increase in the ET rate and disappears when $-\Delta G°$ equals the reorganization energy. Interestingly, as $-\Delta G°$ increases further, a reaction barrier reemerges and the ET rate decreases. This so-called inverted region, illustrated in Figure 1, is well-established and has been experimentally verified.[8−11] However, many systems predicted to exhibit inverted region behavior do not and have ET rates that exceed expected rates by orders of magnitude.[10,12−16] One mechanism used to explain these deviations is the participation of excited states in the ET products, of either vibrational or electronic nature.[14,17−20] Both effectively reduce the exergonicity of the ET process; the case of an electronically excited state is illustrated in Figure 1, in which the barrier can be bypassed by accessing an excited state of the radical anion of the acceptor, $A^{\bullet-}*$. These excited states may have ultrafast nonradiative relaxation pathways, as depicted in Figure 1, providing a very efficient path to the ground state products. Low-lying electronic states are indeed common in the radical anions of many typical electron acceptors, $A^{\bullet-}$.[21,22] Several groups have used time-resolved methods to observe the dynamics of photoinduced ET reactions in the condensed phase and have suggested that electronically excited states of the electron acceptor participate.[23−29] Studies

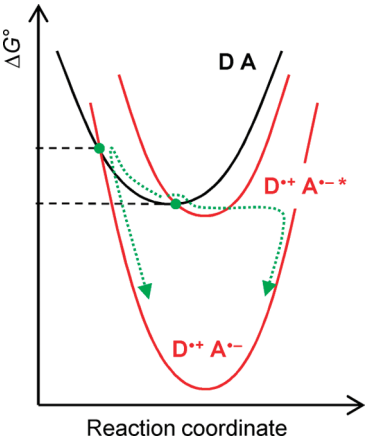

Figure 1. Schematic diagram of the states involved in highly exergonic electron-transfer reactions. In the absence of excited states the reaction encounters a barrier, leading to reduced ET rates for highly exergonic reactions. The presence of an excited state ($D^{\bullet+}A^{\bullet-}*$) offers an alternative pathway with a much reduced reaction barrier. This state can subsequently relax to the ground state, preserving the overall exergonicity of the reaction.

on the dynamics of electronically excited states of typical acceptor molecules in their ET product state (e.g., $A^{\bullet-}$ in Figure 1) have also been performed, indicating that excited states in many systems are short-lived.[30−34] Here, we consider the dynamics of a typical $A^{\bullet-}$ from a gas-phase perspective, providing intrinsic information about the relevant electronic states that could participate in an ET process. Specifically, we show that in the 2,3,5,6-tetrafluoro-7,7,8,

Received: April 25, 2011
Revised: June 14, 2011
Published: June 18, 2011

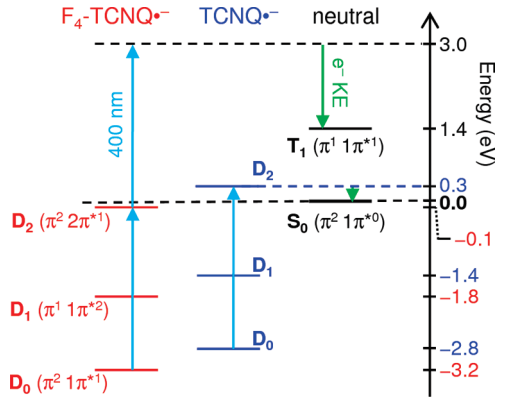

Figure 2. Electronic state diagram of the anionic (red) and neutral (black) states of F_4-TCNQ. Shown for comparison are the anionic states of TCNQ (blue). The presence of the fluorine atoms in F_4-TCNQ stabilizes its anionic states $D_0(1^2B_{2g})$, $D_1(1^2B_{3u})$, and $D_2(2^2B_{3u})$ by 0.4 eV with respect to the analogous nonfluorinated TCNQ anion states. This brings the valence excited D_2 state below the neutral ground state $S_0(^1A_g)$ energy, yielding two vertically bound excited states in F_4-TCNQ$^{\bullet-}$. Also indicated are relevant transitions for the photoelectron spectrum recorded at 400 nm (3.1 eV), shown in Figure 3.

8-tetracyanoquinodimethane radical anion, F_4-TCNQ$^{\bullet-}$, there are two low-lying electronic states that relax to the ground state on sub-200 fs time scales.

F_4-TCNQ is one of the most celebrated electron acceptors,[35] and derivatives of 7,7,8,8-tetracyanoquinodimethane (TCNQ) are widely used.[36,37] It has widespread technological applications as a dopant in organic light emitting diodes[38,39] and in the development of organic molecule based magnetism.[40,41] More generally, the chromophore of TCNQ is the quinone moiety, whose radical anion also possesses low-lying excited states,[42] and plays prominent roles as electron acceptors in bacteria and photosynthesis in green plants.[43] Despite the scientific and technological applications of F_4-TCNQ$^{\bullet-}$, it is surprising that very few studies on the electronic structure of the isolated anion have been reported.

Ab initio quantum calculations indicate that the doublet ground state of the anion (1^2B_{2g}, labeled D_0 in Figure 2) and the singlet ground state of the neutral (^1A_g, labeled S_0) both have D_{2h} symmetry and the anion has a vertical attachment energy of 2.89 eV at the MP4 level of theory.[44] Calculations of low-lying excited states of F_4-TCNQ$^{\bullet-}$ have found at least two anion excited states that are vertically bound with respect to the neutral ground state.[44] With reference to the energy-level diagram in Figure 2, the first is a core-excited[45] state (1^2B_{3u}, labeled D_1) in which a π electron (from the π^2 $1\pi^{*1}$ anion ground state configuration) is promoted into the $1\pi^*$ antibonding orbital ($4b_{2g} \leftarrow 4b_{3u}$), yielding a π^1 $1\pi^{*2}$ configuration. The second is a valence-excited state (2^2B_{3u}, labeled D_2), calculated to be vertically bound relative to the neutral S_0 state by 0.24 eV, and corresponds to the promotion of an electron from the singly occupied $1\pi^*$ orbital of the anion to a higher-lying $2\pi^*$ orbital ($5b_{3u} \leftarrow 4b_{2g}$). An additional state ($1^2A_g$) is calculated to be bound by <0.1 eV, but has a small oscillator strength (see Supporting Information for details). Calculations also indicate that the lowest energy geometries for the anion excited states do not possess D_{2h} symmetry and undergo large geometric rearrangement following vertical excitation from D_0. The spectroscopy and electronic structure of F_4-TCNQ$^{\bullet-}$ are similar to those of TCNQ$^{\bullet-}$, for which a gas-phase absorption spectrum[22] and a photoelectron spectrum[46] have been measured, and they have been the focus of a number of theoretical studies.[47−49] Below, we make the comparison between F_4-TCNQ$^{\bullet-}$ and TCNQ$^{\bullet-}$ to provide additional insight into the relative locations of electronic states.

To directly probe the relaxation dynamics of excited states in isolated F_4-TCNQ$^{\bullet-}$, we use time-resolved photoelectron spectroscopy and specifically imaging.[50−52] Changes within the measured photoelectron kinetic energy spectrum as a function of pump−probe delay (Δt) can be used to obtain information about the electronic state populations and vibrational dynamics. The aim of the present study is to determine how effective anionic excited states of a prototypical electron acceptor, F_4-TCNQ, are at accepting an electron and subsequently guiding this to the electronic ground state of the anion.

2. EXPERIMENTAL DETAILS

A detailed description of the experimental apparatus has been given elsewhere.[46,53] Briefly, anions are produced via electrospray ionization of a 1 mM solution of F_4-TCNQ in acetonitrile through a stainless steel needle biased at −2.5 kV. The anion aerosol then enters a differentially pumped vacuum chamber through a heated stainless steel capillary. Anions are subsequently stored inside a radio frequency ring electrode trap and ejected at 500 Hz repetition rate into a collinear Wiley−McLaren type time-of-flight mass spectrometer.[54] The internal energy of the anions is approximately room temperature as the ions are thermalized in the trap. Ions are accelerated and a packet of F_4-TCNQ$^{\bullet-}$ is mass selected and focused by a pair of Einzel lenses into the interaction region. The F_4-TCNQ$^{\bullet-}$ ion bunch is intersected by femtosecond laser pulses in the center of a velocity-map imaging (VMI) arrangement.[55] The VMI arrangement allows for the velocity vectors of the emitted electrons to be measured by projecting the three-dimensional (3D) photoelectron cloud onto a two-dimensional position-sensitive detector, comprised of a pair of microchannel plates coupled to a phosphor screen. A charge-coupled device is then used to collect images of the photoelectrons striking the phosphor. The 3D photoelectron cloud is reconstructed using a polar onion-peeling algorithm.[56] From this, the photoelectron spectrum, as well as the angular distribution of photoelectrons, is obtained.

Laser pulses are derived from a commercial femtosecond oscillator and amplifier system (Spectra Physics Tsunami and Spitfire XP Pro), producing fundamental 800 nm pulses of 35 fs duration at a 1 kHz repetition rate. Radiation at 400 nm is produced by frequency doubling of the fundamental in a β-barium borate (BBO) crystal. Radiation at 1200 nm is generated in an optical parametric amplifier (TOPAS, Light Conversion). The optical parametric amplifier is also used to generate 500 nm by sum-frequency mixing its signal output at 1330 nm with the 800 nm fundamental in a type II BBO crystal. Probe pulses are delayed relative to pump pulses using a computer controlled optical delay line (Physik-Instrumente).

Power densities at all wavelengths used are on the order of 1×10^{10} W cm^{-2}. The temporal resolution of the experiment is determined by the laser pulses and depends on the combination of pump and probe wavelengths used. The cross-correlation between 400 and 1200 nm is measured to be 50 fs, between 800 and 500 nm it is estimated to be 110 fs, and between 400 and 500 nm it is 130 fs. Photoelectron images are typically collected for 2×10^5 laser shots at each optical delay.

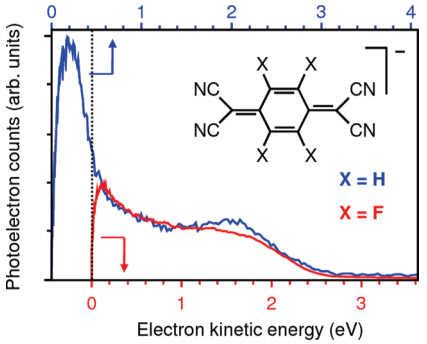

Figure 3. Photoelectron spectra of $TCNQ^{\bullet -}$ (blue, top scale)[46] and F_4-$TCNQ^{\bullet -}$ (red, bottom scale) recorded at 3.1 eV (400 nm) photon energy. The spectrum of $TCNQ^{\bullet -}$ has been shifted by −0.4 eV with respect to that for F_4-$TCNQ^{\bullet -}$, illustrating the effect of the additional fluorine atoms. The unbound $D_2(2^2B_{3u})$ state in $TCNQ^{\bullet -}$ is bound in F_4-$TCNQ^{\bullet -}$ (see Figure 2).

3. RESULTS AND DISCUSSION

3.1. Photoelectron Spectrum at 3.1 eV. To experimentally probe the electronic structure of F_4-$TCNQ^{\bullet -}$, the photoelectron spectrum taken at 400 nm (3.1 eV) is compared with that of $TCNQ^{\bullet -}$ under identical conditions,[46] as shown in Figure 3. A 3.1 eV photon is resonant with the $D_2 \leftarrow D_0$ transition in both $TCNQ^{\bullet -}$ and F_4-$TCNQ^{\bullet -}$.[57,58] In the $TCNQ^{\bullet -}$ spectrum (blue line in Figure 2), the prominent feature at 0.2 eV can be assigned to autodetachment from the D_2 state, leaving the neutral in the S_0 ground state: $D_2(\pi^2\, 2\pi^{*1}) \rightarrow S_0(\pi^2\, 2\pi^{*0}) + e^-$. This is in stark contrast to the photoelectron spectrum of F_4-$TCNQ^{\bullet -}$, which reveals no such peak. Only the high energy shoulder of this feature is observed in the photoelectron spectrum, which indicates that the D_2 excited state is bound with respect to electron loss. Based on the comparison between the two spectra and the fact that the absorption spectra of $TCNQ^{\bullet -}$ and F_4-$TCNQ^{\bullet -}$ are very similar,[57,58] it is evident that the presence of the fluorine atoms in F_4-$TCNQ^{\bullet -}$ has stabilized all the anionic states by approximately 0.4 eV with respect to the electronic states of $TCNQ^{\bullet -}$. This is indicated in the energy diagram in Figure 2 where the S_0 states of neutral TCNQ and F_4-TCNQ are referenced as 0 eV.

The broad photoelectron feature at high energy can be attributed to a two-photon resonance-enhanced photodetachment process. For $TCNQ^{\bullet -}$, where more detailed calculations[44,48] and experimental data[46,53] are available, the dominant configuration of the D_2 state is $\pi^2\, 2\pi^{*1}$; however, there is also a ~10% contribution from the core-excited $\pi^1\, 1\pi^{*2}$ state. It is this latter contribution that allows the photoelectron spectrum to be rationalized in terms of Koopmans' correlations, which require that the neutral state must have the same electronic configuration as the initial anionic state excluding the photodetached electron.[59] Removal of a $1\pi^*$ electron from the core-excited contribution will leave the neutral in the T_1 state with its $\pi^1\, 1\pi^{*1}$ configuration. For $TCNQ^{\bullet -}$, this channel appears to have a very large cross section. We apply the same argument to F_4-$TCNQ^{\bullet -}$ and have carried out time-dependent density function theory calculations (see Supporting Information for details) to show that indeed there is a contribution from core-excited orbitals. Energetically, the total photon energy imparted to the system amounts to 6.2 eV, while the electron affinity is approximately 3.2 eV and the singlet−triplet gap in the neutral is about 1.4 eV, resulting in photoelectrons centered around 1.6 eV, as observed in the measured spectrum. Interestingly,

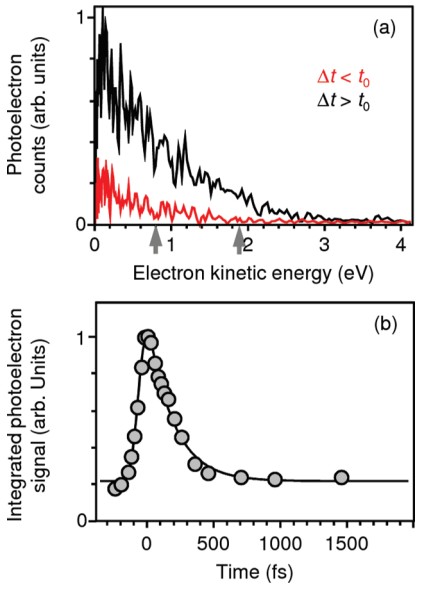

Figure 4. Time-resolved dynamics of the $D_1(1^2B_{3u})$ excited state of F_4-$TCNQ^{\bullet -}$, excited at 800 nm (1.5 eV) and probed at 500 nm (2.5 eV). (a) Photoelectron spectra recorded at negative (red) and positive (black) pump−probe delays. Gray arrows indicate the maximum kinetic energy expected for a one- or two-photon photodetachment from the D_1 state with the 2.5 eV probe. (b) Total integrated photoelectron signal as a function of pump−probe delay (gray circles) and fit (solid line) to yield a lifetime of 190 fs.

there is no clear indication of the detachment from D_2 leaving the neutral in S_0, which would produce photoelectrons up to 3.0 eV, in either F_4-$TCNQ^{\bullet -}$ or $TCNQ^{\bullet -}$. On the basis of the dominant $\pi^2\, 2\pi^{*1}$ electronic configuration of the D_2 state, one would anticipate that this is the prevailing photodetachment channel, but it appears to possess a very small cross section.

3.2. Ultrafast Relaxation Dynamics of the D_1 Core-Excited State. The solution-phase absorption spectra of F_4-$TCNQ^{\bullet -}$ suggests that the D_1 state lies about 1.4 eV above the anion ground state.[58] To monitor its relaxation dynamics, the D_1 state is excited at 800 nm (1.5 eV) and probed at variable delays, Δt, with 500 nm (2.5 eV) femtosecond pulses. With reference to Figure 2, the probe energy is sufficient to detach an electron from the D_1 state and produce neutral ground state F_4-TCNQ. Figure 4a shows two representative photoelectron spectra, taken at negative ($\Delta t < t_0$, probe−pump) and positive ($\Delta t > t_0$, pump−probe) delays with respect to the temporal overlap of pump and probe, t_0. In the absence of the pump pulse, the probe has insufficient energy to detach an electron from the D_0 state and no photoelectron signal is expected at negative delays. The small signal observed for $\Delta t < t_0$ is attributed to nonresonant multiphoton detachment processes. At positive delays, a broad photoelectron spectrum is observed, extending beyond 2 eV. Detachment from the D_1 to the S_0 neutral state with 2.5 eV photons will produce photoelectrons with kinetic energies up to 0.8 eV (as indicated by a vertical gray arrow in Figure 4a), and we attribute the low energy photoelectron signal to this detachment channel. The higher energy electrons are assigned to two-photon absorption from the D_1 state, which accesses the T_1 state in the neutral, producing photoelectrons with kinetic energies up to 1.9 eV. The fact that electrons are observed with higher kinetic energy is probably due to the fact that the first photon imparts a significant amount of

dx.doi.org/10.1021/jp2038202 |J. Phys. Chem. A 2011, 115, 8369–8374

vibrational energy in the excited state, so the second photon which accesses the ground state contains a large contribution from hot bands. Despite the requirement of two probe photons, the sizable intensity of the higher energy feature relative to the single photon detachment channel can again be rationalized in terms of Koopmans' correlations. Removal of a single $1\pi^*$ electron from the anionic $D_1(\pi^1\ 1\pi^{*2})$ state does not correlate with the $S_0(\pi^2\ 1\pi^{*0})$, but does correlate with the excited $T_1(\pi^1\ 1\pi^{*1})$ state of the neutral. The much larger cross sections for this process mean that, despite the fact that two photons are needed to access T_1, it is of comparable intensity to the one-photon process accessing S_0.

The relaxation dynamics of the D_1 state are studied by considering the total integrated photoelectron signal as a function of pump−probe delay. This is shown in Figure 4b and indicates a very rapid decay of the D_1 excited state population. The data are fit to a convolution between the Gaussian pump−probe cross-correlation and an exponential first order decay,[46] the result of which is shown as a solid line in Figure 4b. The fit yields a characteristic lifetime of the D_1 excited state of 190 ± 65 fs. The lifetime is a direct measure of the D_1 population kinetics, and the mechanism is assigned to direct internal conversion from the D_1 state to the vibrationally hot D_0 ground state.

3.3. Ultrafast Relaxation Dynamics of the D_2 Valence-Excited State. From an electron acceptor point of view, perhaps the more relevant excited state is the D_2 state: in Koopmans' picture, the $D_2(\pi^2\ 2\pi^{*1})$ state corresponds to the addition of a single electron to the neutral, producing an anion without any core excitations. Furthermore, from the perspective of an isolated system, the D_2 lies very close in energy to the neutral ground state, so a quasi-free electron could be captured by the D_2 anionic state.

The dynamics of the D_2 state are studied by exciting it using a 400 nm (3.1 eV) pump pulse and probing the ensuing dynamics using a 1200 nm (1.0 eV) probe pulse. The probe is sufficient to detach an electron from D_2 to produce neutrals in the S_0 state, with which the D_2 state is correlated in Koopmans' picture. At negative time delays, the photoelectron spectrum (red trace in Figure 5a) is identical to the one-color photoelectron spectrum recorded at 3.1 eV (Figure 3), as the 1.0 eV probe photon is not resonant with any transition and does not possess sufficient energy to detach an electron from the D_0 state. At positive time delays we observe a small increase in the photoelectron yield at low kinetic energies (black trace in Figure 5a). This signal increase arises as a result of photodetachment from the D_2 state to the S_0 state, producing electrons with a maximum kinetic energy of 0.9 eV (indicated by a vertical gray arrow in Figure 5a). The pump−probe signal is however concentrated at lower kinetic energy, indicating that the neutral is produced with some internal energy. It is also worth noting that the increase in signal is unexpectedly small, which can be explained in terms of the relatively small cross section for photodetachment to the S_0 state as discussed previously.

Figure 5b shows the integrated photoelectron signal between 0 and 0.5 eV as a function of pump−probe delay. A sharp increase in total signal is observed around t_0 followed by an exceptionally fast decay. A fit to these data using the same procedure as that used for the D_1 state dynamics yields a lifetime of 57 ± 30 fs for the D_2 excited state. As the change in photoelectron signal only amounts to a maximum of 10%, we have also analyzed the photoelectron anisotropy in order to confirm the fast relaxation process. We have recently shown that this can be used to provide excited state dynamics,[53] and in Figure 5c, the variation of the

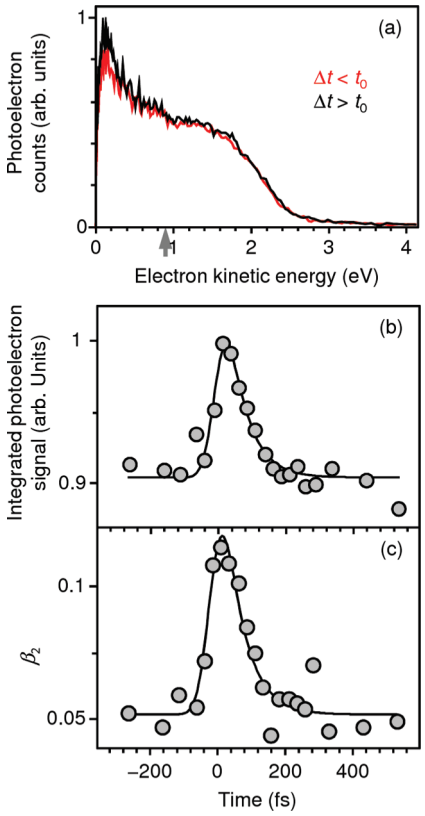

Figure 5. Time-resolved dynamics of the $D_2(2^2B_{3u})$ excited state of F_4-$TCNQ^{\bullet-}$, excited at 400 nm (3.1 eV) and probed at 1200 nm (1.0 eV). (a) Photoelectron spectra recorded at negative (red) and positive (black) pump−probe delays. The gray arrow indicates the maximum kinetic energy expected for photodetachment from the D_2 state (leaving the neutral in its $S_0(^1A_g)$ ground state) with a 1.0 eV probe photon. (b) Integrated photoelectron signal from 0 to 0.5 eV as a function of pump−probe delay (gray circles) and fit (solid line). (c) Measured photoelectron anisotropy parameter, β_2, associated with the time-dependent photoelectron signal in (b) (gray circles) and fit (solid line).

photoelectron anisotropy parameter (β_2) is plotted as a function of pump−probe delay.[60] Although β_2 values have a large systematic error (on the order of ±0.1 in the current experiment) and have an error associated with their measurement obtained by fitting the photoelectron images,[56] they are much less sensitive to overall intensity fluctuations, which are the primary source of noise in our experiment. A fit to these data yields a lifetime of 58 ± 30 fs for the D_2 state, in excellent agreement with the time constant extracted from the integrated photoelectron signal.

If the observed decay can be assigned to internal conversion, the D_2 state can either relax directly down to the D_0 ground state or, alternatively, relax to the D_1 state and then to the D_0 ground state. In an attempt to gain additional insight into these dynamics, the time-resolved photoelectron spectra using a 400 nm (3.1 eV) pump and 500 nm (2.5 eV) probe have also been recorded. Photoelectron spectra, from which a spectrum at $\Delta t < t_0$ has been subtracted, are plotted as a false-color intensity plot in Figure 6. Using the 2.5 eV probe, transient population in the D_1 state should be observable if it was populated from the D_2 state via internal conversion. As the lifetime of the D_1 is relatively slow (~200 fs) compared with that of the D_2 state, we would expect to observe a rise in the signal in the time-resolved spectra that is similar in appearance to the spectrum presented in Figure 4a. The

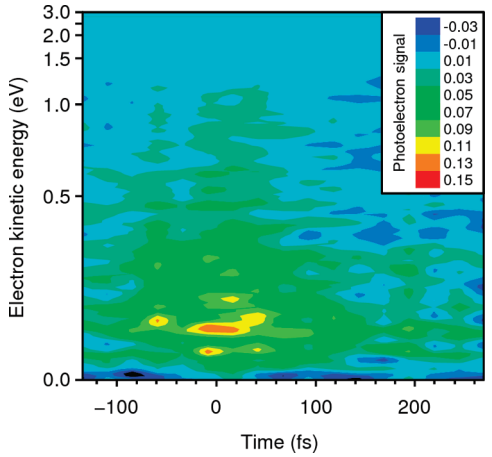

Figure 6. Contour (false-color intensity) plot of time-resolved photoelectron spectra of the $D_2(2^2B_{3u})$ excited state of F_4-$TCNQ^{\bullet -}$, excited at 400 nm (3.1 eV) and probed at 500 nm (2.5 eV). The lack of significant spectral shifting with delay suggests minimal geometric changes.

rise time of this feature would be characteristic of the D_2 relaxation time, and a subsequent decrease would occur on a time scale of the D_1 state (Figure 4b). No such signal is observed and our data suggest that the D_1 state is not populated, although we point out that the cross section for detachment from the D_1 to the S_0 is expected to be small, as observed in Figure 4a. From Figure 6, a lifetime of 89 ± 55 fs is extracted for the D_2 state. Given the reduced time resolution using the 500 nm probe (130 fs cross-correlation), the measured lifetime is commensurate with the 60 fs D_2 lifetime measured using the 1200 nm probe and supports the argument that the D_1 state is not populated.

Figure 6 furthermore shows that there is no noticeable change in kinetic energy of the time-resolved feature. Such spectral shifts are a measure of changing Franck−Condon factors and are indicative of vibrational wave packet dynamics on the excited state. The fact that no such shifts are observed suggests that there is minimal geometric change occurring on the D_2 excited state before the population decays.

4. DISCUSSION

Excited state lifetimes of sub-100 fs are typically attributed to relaxation through conical intersections. In the case of the D_2 state, we invoke a similar situation because the internal conversion time scale cannot otherwise be explained in terms of a simple golden rule expression. Calculations by the Simons group[44] indicate that the minimum energy structures of the excited states are not of D_{2h} symmetry, although they are formed in this geometry following a vertical transition from the D_0 state. The initial motion on the D_2 excited state involves a mode of b_{3u} symmetry, in which the $C(CN)_2$ groups bend out of the plane of the carbon ring, while the F atoms bend in the opposite direction. The final F_4-$TCNQ^{\bullet -}$ lowest energy structure on the D_2 state was calculated to have a vertical detachment energy of 2.7 eV to the neutral S_0 ground state (at the MP2 level of theory). In the time-resolved photoelectron spectra, such dynamics would be revealed by shifts in the kinetic energy of peaks arising from photoelectrons produced via detachment from the D_2 state using either 1200 or 500 nm. As evidenced in Figure 6, no such dynamics are observed. Moreover, the time scale required to impose the predicted geometric deformation is much longer than the observed time scale of 60 fs. Our results thus suggest that the D_2 excited state rapidly relaxes via a conical intersection to the D_0 ground state and hence cannot explore the full excited state potential energy surface. A similar situation arises in the core excited D_1 state, which is calculated to become unstable with respect to electron loss at its minimum energy structure. Internal conversion from the D_1 state naturally leaves the anion in its ground state.

The observation that the excited states, and in particular the D_2 state, are extremely short-lived enhances the ability of F_4-$TCNQ^{\bullet -}$ as an electron acceptor. Considering the isolated system, the neutral F_4-TCNQ can readily accept a very low energy electron via the D_2 state and almost instantly transfer this excess charge into the ground state. Once in the D_0 ground state internal vibrational relaxation will redistribute the excess energy into the vibrational modes of the anion ground state. In the condensed phase, this excess energy can then be lost to the surrounding environment.

The accessibility of anionic excited states of the acceptor allows for near-barrierless ET reactivity as suggested in Figure 1, in which the conical intersection is along an internal coordinate, not shown in Figure 1. The large internal vibrational energy required to access the crossing between reactants and products is effectively transformed into electronic energy. Moreover, the Franck−Condon factors can be much more favorable in the case of electronically excited states, requiring much smaller geometric changes to accommodate the charge. In the case of F_4-$TCNQ^{\bullet -}$, this excited state then rapidly relaxes into the anion ground state via a conical intersection, yielding a very efficient pathway for ET that bypasses the activation barrier between the neutral ground state and the anion ground state.

More generally, low-lying excited states have also been observed in the *p*-benzoquinone radical anion, which shares the same quinone chromophore with F_4-$TCNQ^{\bullet -}$ and possesses similar excited state characteristics.[42] In the isolated *p*-benzoquinone radical anion, these excited anion states are unbound with respect to the neutral ground state. Based on the spectral width of resonances observed in the photodetachment spectra of this radical, it was argued that these excited states are likely to have very short lifetimes and could lead to rapid internal conversion to the ground state.[42] Excited states of the quinone moiety have indeed been invoked to explain dramatic deviations from ET theory in the inverted region.[15] Our results suggest that this may be due to the availability of anionic excited states and their extremely fast relaxation, thus enabling the ground state to be formed prior to electron back-transfer.[16] We are currently investigating the dynamics in quinone derivatives in an attempt to confirm this and hope that the presented results will inspire theoretical work aimed at uncovering the mechanistic details of the conical intersections responsible for our observations.

5. CONCLUSION

We have presented the photoelectron spectrum and ultrafast dynamics of F_4-$TCNQ^{\bullet -}$ in the gas phase. The presence of two bound excited states of the anion is observed, and their relaxation dynamics are measured using time-resolved photoelectron spectroscopy. Both core-excited and valence-excited states exhibit lifetimes that are shorter than 200 fs. The D_2 excited state is particularly short-lived (60 fs), with the relaxation dynamics likely to involve a conical intersection with the D_0 ground state. Excited states of acceptor radical anions are believed to play an

important role in ET reactions, and the study of the isolated anion allows the relaxation dynamics of these systems to be studied directly. Neutral F_4-TCNQ can readily accept an excess electron into the D_2 state and deactivate this to the ground anion state within 100 fs. We believe these electronic characteristics could be a general feature of the quinone family that explains their excellent electron-accepting abilities.

■ ASSOCIATED CONTENT

Supporting Information. Details of calculations on the excited state contributions and oscillator strengths. This material is available free of charge via the Internet at http://pubs.acs.org.

■ AUTHOR INFORMATION

Corresponding Author
*E-mail: j.r.r.verlet@durham.ac.uk.

■ ACKNOWLEDGMENT

We are grateful to Durham University and the EPSRC for funding under Grant EP/D073472/1.

■ REFERENCES

(1) Renger, G.; Renger, T. *Photosynth. Res.* **2008**, *98*, 53–80.
(2) Chitnis, P. R. *Annu. Rev. Plant Physiol. Plant Mol. Biol.* **2001**, *52*, 593–626.
(3) Yu, G.; Gao, J.; Hummelen, J. C.; Wudl, F.; Heeger, A. J. *Science* **1995**, *270*, 1789–1791.
(4) Moser, C. C.; Keske, J. M.; Warncke, K.; Farid, R. S.; Dutton, P. L. *Nature* **1992**, *355*, 796–802.
(5) Barbara, P. F.; Meyer, T. J.; Ratner, M. A. *J. Phys. Chem.* **1996**, *100*, 13148–13168.
(6) Nitzan, A. *Annu. Rev. Phys. Chem.* **2001**, *52*, 681–750.
(7) Marcus, R. A.; Sutin, N. *Biochim. Biophys. Acta* **1985**, *811*, 265–322.
(8) Wasielewski, M. R.; Niemczyk, M. P.; Svec, W. A.; Pewitt, E. B. *J. Am. Chem. Soc.* **1985**, *107*, 1080–1082.
(9) Creutz, C.; Sutin, N. *J. Am. Chem. Soc.* **1977**, *99*, 241–243.
(10) Closs, G. L.; Miller, J. R. *Science* **1988**, *240*, 440–447.
(11) Miller, J. R.; Beitz, J. V.; Huddleston, R. K. *J. Am. Chem. Soc.* **1984**, *106*, 5057–5068.
(12) Beitz, J. V.; Miller, J. R. *J. Chem. Phys.* **1979**, *71*, 4579–4595.
(13) Indelli, M. T.; Ballardini, R.; Scandola, F. *J. Phys. Chem.* **1984**, *88*, 2547–2551.
(14) Rehm, D.; Weller, A. *Isr. J. Chem.* **1970**, *8*, 259.
(15) Closs, G. L.; Calcaterra, L. T.; Green, N. J.; Penfield, K. W.; Miller, J. R. *J. Phys. Chem.* **1986**, *90*, 3673–3683.
(16) Rehm, D.; Weller, A. *Ber. Bunsen-Ges. Phys. Chem.* **1969**, *73*, 834.
(17) Suppan, P. The Marcus inverted region. In *Photoinduced Electron Transfer IV*; Mattay, J., Ed.; Topics in Current Chemistry 163; Springer: Berlin/Heidelberg, 1992; pp 95−130.
(18) Marcus, R. A.; Siders, P. *J. Phys. Chem.* **1982**, *86*, 622–630.
(19) Mataga, N.; Chosrowjan, H.; Taniguchi, S. *J. Photochem. Photobiol., C* **2005**, *6*, 37–79.
(20) Barbara, P. F.; Walker, G. C.; Smith, T. P. *Science* **1992**, *256*, 975–981.
(21) Shida, T.; Haselbach, E.; Bally, T. *Acc. Chem. Res.* **1984**, *17*, 180–186.
(22) Brinkman, E. A.; Gunther, E.; Schafer, O.; Brauman, J. I. *J. Chem. Phys.* **1994**, *100*, 1840–1848.
(23) Petersson, J.; Eklund, M.; Davidsson, J.; Hammarström, L. *J. Phys. Chem. B* **2010**, *114*, 14329–14338.
(24) Morandeira, A.; Engeli, L.; Vauthey, E. *J. Phys. Chem. A* **2002**, *106*, 4833–4837.
(25) Muller, P.-A.; Vauthey, E. *J. Phys. Chem. A* **2001**, *105*, 5994–6000.
(26) Pagès, S.; Lang, B.; Vauthey, E. *J. Phys. Chem. A* **2003**, *108*, 549–555.
(27) Vauthey, E. *J. Photochem. Photobiol., A* **2006**, *179*, 1–12.
(28) Vân Anh, N.; Schlosser, F.; Groeneveld, M. M.; van Stokkum, I. H. M.; Würthner, F.; Williams, R. M. *J. Phys. Chem. C* **2009**, *113*, 18358–18368.
(29) Lukas, A. S.; Zhao, Y.; Miller, S. E.; Wasielewski, M. R. *J. Phys. Chem. B* **2002**, *106*, 1299–1306.
(30) Brodard, P.; Sarbach, A.; Gumy, J.-C.; Bally, T.; Vauthey, E. *J. Phys. Chem. A* **2001**, *105*, 6594–6601.
(31) Gumy, J.-C.; Vauthey, E. *J. Phys. Chem. A* **1997**, *101*, 8575–8580.
(32) Hope, M. J.; Higlett, M. P.; Andrews, D. L.; Meech, S. R.; Hands, I. D.; Dunn, J. L.; Bates, C. A. *Chem. Phys. Lett.* **2009**, *474*, 112–114.
(33) Mandal, D.; Tahara, T.; Meech, S. R. *J. Phys. Chem. B* **2003**, *108*, 1102–1108.
(34) Gosztola, D.; Niemczyk, M. P.; Svec, W.; Lukas, A. S.; Wasielewski, M. R. *J. Phys. Chem. A* **2000**, *104*, 6545–6551.
(35) Wheland, R. C.; Martin, E. L. *J. Org. Chem.* **1975**, *40*, 3101–3109.
(36) Emge, T. J.; Bryden, W. A.; Wiygul, F. M.; Cowan, D. O.; Kistenmacher, T. J.; Bloch, A. N. *J. Chem. Phys.* **1982**, *77*, 3188–3197.
(37) Fourmigue, M.; Perrocheau, V.; Clerac, R.; Coulon, C. *J. Mater. Chem.* **1997**, *7*, 2235–2241.
(38) Pfeiffer, M.; Leo, K.; Zhou, X.; Huang, J. S.; Hofmann, M.; Werner, A.; Blochwitz-Nimoth, J. *Org. Electron.* **2003**, *4*, 89–103.
(39) Walzer, K.; Maennig, B.; Pfeiffer, M.; Leo, K. *Chem. Rev.* **2007**, *107*, 1233–1271.
(40) Miller, J. S. *Dalton Trans.* **2006**, 2742–2749.
(41) Lopez, N.; Zhao, H.; Prosvirin, A. V.; Chouai, A.; Shatruk, M.; Dunbar, K. R. *Chem. Commun.* **2007**, 4611–4613.
(42) Schiedt, J.; Weinkauf, R. *J. Chem. Phys.* **1999**, *110*, 304–314.
(43) Klinman, J. P.; Mu, D. *Annu. Rev. Biochem.* **1994**, *63*, 299–344.
(44) Sobczyk, M.; Skurski, P.; Simons, J. *J. Phys. Chem. A* **2003**, *107*, 7084–7091.
(45) Here "core-excited" refers to an excitation of an electron residing in a filled energy level, below the singly occupied $4b_{2g}$ valence state.
(46) Roberts, G. M.; Lecointre, J.; Horke, D. A.; Verlet, J. R. R. *Phys. Chem. Chem. Phys.* **2010**, *12*, 6226–6232.
(47) Zanon, I.; Pecile, C. *J. Phys. Chem.* **1983**, *87*, 3657–3664.
(48) Skurski, P.; Gutowski, M. *THEOCHEM* **2000**, *531*, 339–348.
(49) Makowski, M.; Pawlikowski, M. T. *Int. J. Quantum Chem.* **2006**, *106*, 1736–1748.
(50) Stolow, A.; Bragg, A. E.; Neumark, D. M. *Chem. Rev.* **2004**, *104*, 1719–1758.
(51) Suzuki, T. *Annu. Rev. Phys. Chem.* **2006**, *57*, 555–592.
(52) Verlet, J. R. R. *Chem. Soc. Rev.* **2008**, *37*, 505–517.
(53) Lecointre, J.; Roberts, G. M.; Horke, D. A.; Verlet, J. R. R. *J. Phys. Chem. A* **2010**, *114*, 11216–11224.
(54) Wiley, W. C.; McLaren, I. H. *Rev. Sci. Instrum.* **1955**, *26*, 1150–1157.
(55) Eppink, A. T. J. B.; Parker, D. H. *Rev. Sci. Instrum.* **1997**, *68*, 3477–3484.
(56) Roberts, G. M.; Nixon, J. L.; Lecointre, J.; Wrede, E.; Verlet, J. R. R. *Rev. Sci. Instrum.* **2009**, *80*, 053104.
(57) Haller, I.; Kaufman, F. B. *J. Am. Chem. Soc.* **1976**, *98*, 1464–1468.
(58) Panja, S.; Kadhane, U.; Andersen, J. U.; Holm, A. I. S.; Hvelplund, P.; Kirketerp, M.-B. S.; Nielsen, S. B.; Stochkel, K.; Compton, R. N.; Forster, J. S.; Kilsa, K.; Nielsen, M. B. *J. Chem. Phys.* **2007**, *127*, 124301.
(59) Koopmans, T. *Physica* **1934**, *1*, 104–113.
(60) When analyzing the photoelectron images, the angular anisotropy was fit to the usual angular distribution formula (see refs 50 and 51) with even Legendre polynomial up to $n = 4$. From this, the β_4 anisotropy parameters were zero and showed no time dependence.